JOURNAL OF RAMAN SPECTROSCOPY
J. Raman Spectrosc. 2002; **33**: 301–308
Published online in Wiley InterScience (www.interscience.wiley.com). DOI: 10.1002/jrs.863

JRS

UV Raman spectroscopic study on the phase transformation of ZrO_2, Y_2O_3–ZrO_2 and SO_4^{2-}/ZrO_2

Can Li* and Meijun Li

State Key Laboratory of Catalysis, Dalian Institute of Chemical Physics, Chinese Academy of Sciences, Dalian 116023, China

Received 2 July 2001; Accepted 14 February 2002

The phase evolution of zirconia (ZrO_2), sulfated zirconia (SO_4^{2-}/ZrO_2) and yttrium oxide incorporated zirconia (Y_2O_3–ZrO_2) from the tetrahedral phase to the monoclinic phase was studied using UV Raman spectroscopy, visible Raman spectroscopy and x-ray diffraction (XRD). It is clearly observed that there are discrepancies between the results from the UV Raman spectra, visible Raman spectra and XRD patterns. The phase change from tetragonal to monoclinic is always earlier or at lower calcination temperatures as observed by UV Raman spectroscopy than by visible Raman spectroscopy and XRD. UV Raman spectroscopy is found to be more sensitive at the surface region while visible Raman spectroscopy and XRD supply the information mainly from the bulk. The inconsistency in the results from the three techniques suggests that the phase transformation of zirconia starts from its surface region and then gradually develops into its bulk. For SO_4^{2-}/ZrO_2 and Y_2O_3–ZrO_2, the transformation from the tetragonal to the monoclinic phase is significantly retarded owing to the presence of the sulfated groups and the yttrium oxide. Particularly, the tetragonal phase of Y_2O_3–ZrO_2 can be maintained up to 800 °C although its phase at the surface region changed into monoclinic at 500 °C.

INTRODUCTION

Raman spectroscopy has been used in catalysis studies since the 1970s and it was expected that Raman spectroscopy would develop info one of the most useful techniques for the characterization of catalytic materials and catalytic reactions.[1–5] Although Raman spectroscopy has a number of potential applications in catalysis research, it is not as widely used in catalytic studies as was expected. The main limitations are its relatively low sensitivity and fluorescence interference.[6] Fluorescence interference could be avoided by shifting the excitation laser from the visible region usual for conventional Raman spectroscopy to the UV region (below 300 nm) without fluorescence interference.

Since 1995, we have carried out the UV Raman spectroscopic studies of catalysts[7] and studied sulfated zirconia,[8] coked catalysts,[9,10] zeolites and alumina-supported oxides[11–13] that all have a strong fluorescence background in their visible Raman spectra, but are free of fluorescence interference in the UV Raman spectra. Hence UV Raman spectroscopy opens up the possibility of characterizing those catalysts which are difficult to study by conventional visible Raman spectroscopy.

For UV Raman spectroscopy, not only is fluorescence avoided, but also the sensitivity can be improved.[14] The Raman scattering intensity can be enhanced when the excitation laser is shifted from the visible (for conventional Raman) or near-infrared (for Fourier transform Raman) to the UV region because the Raman scattering is proportional to $1/\lambda^4$ (where λ is the wavelength of the scattering light, approximately that of the excitation laser). Furthermore, the Raman scattering can be greatly enhanced by the resonance Raman effect when the UV laser falls in the region of the electronic absorption of the samples.

Zirconia is an important material, being widely used as a catalyst and catalyst support and also as a ceramic.[15–20] Zirconia exhibits three different phases: monoclinic (m-ZrO_2), tetragonal (t-ZrO_2) and cubic (c-ZrO_2). t-ZrO_2 is a metastable phase of ZrO_2 at low temperatures and it changes into m-ZrO_2 at elevated temperatures.[16,21,22] Metastable t-ZrO_2 can be obtained by thermal treatment of suitable starting materials (zirconium salts, zirconium alkoxides or zirconium hydroxide).[15,16,22,23] Stabilized t-ZrO_2 is important for ceramics and sulfated zirconia catalysts. However, the phase transformation from the metastable tetragonal phase to the monoclinic phase of crystalline ZrO_2 prevents its applications over a broad temperature range. Many studies[24–30] have addressed the factors that affect

*Correspondence to: Can Li, State Key Laboratory of Catalysis, Dalian Institute of Chemical Physics, Chinese Academy of Sciences, Dalian 116023, China. E-mail: canli@dicp.ac.cn, Home Page: http://www.canli.dicp.ac.cn
Contract/grant sponsor: National Science Foundation of China; Contract/grant numbers: 29625305; 20073045.
Contract/grant sponsor: State Key Project for Basic Research, Ministry of Science and Technology; Contract/grant number: G1999022407.

JRS

the phase transformation of tetragonal zirconia. However, past investigations provided the information mainly on the bulk of ZrO_2. The structure change in the surface region of zirconia particles during phase transformation has not been well investigated. We believe that any change in the surface region will make a large difference in the phase change of the bulk, and is associated with the evolution of the phase from tetragonal to monoclinic. However, the mechanism of the phase change is not clearly understood. In addition, it has been reported that the tetragonal phase of zirconia can be stabilized when some additives (e.g. Y_2O_3[31]) or adsorbed species (e.g. SO_4^{2-}[2,32,33]) are present.

Haase and Sauer[33] studied the structure of sulfur species on the surface of t-ZrO_2 by periodic plane wave pseudopotential calculations based on density functional theory. They suggested that the most stable configurations are a tridentate sulfate anion on the (101) surface and an SO_3 complex on the (001) surface of ZrO_2. However, it is still not clear how the Y_2O_3 and SO_4^{2-} stabilize the tetragonal phase of ZrO_2. In this paper, we present our recent results on UV Raman spectroscopic studies on the phase transformation of zirconia, sulfated zirconia and yttrium oxide doped zirconia. It is found that UV Raman spectroscopy is a surface-sensitive technique for zirconia because zirconia has UV absorption. The UV Raman spectra together with visible Raman spectra and x-ray diffraction (XRD) patterns indicate that the phase transformation starts from the surface region of the particle and then extends into the bulk at elevated calcination temperatures.

EXPERIMENTAL

UV Raman spectroscopy

The UV Raman spectra were recorded on a laboratory made UV Raman spectrograph, which was designed especially for *in situ* characterization of catalysts and materials under working conditions. The spectrograph was composed of four parts: the excitation sources, light collection system for Raman scattering, spectrograph and signal detection and data acquisition.

The UV laser sources were a Coherent Innova 300 Fred 300 cw UV laser equipped with an intracavity frequency-doubling system using a BBO crystal to produce SHG (second harmonic generation) outputs at different wavelengths: 229, 238, 244, 257 and 264 nm. The 244 and 257 nm lines are the strongest ones and their power can be over 100 mW. A line at 325 nm is from an He–Cd laser with an output of 25 mW. The UV Raman spectrograph system was set up with a UV-sensitive CCD (Spex) and a triplemate (1877D, Jobin Yvon-Spex). The slit width was about 100–200 μm. The spectral resolution was estimated to be 4.0 cm^{-1} at a slit width of 100 μm. The power of the UV laser lines, measured at the samples, was below 2.0 mW for 244.0 nm and 4.0 mW for 325.0 nm radiation. Samples were mounted in a spinning holder to avoid thermal damage during the spectrum scanning, which usually takes about 5 min. The spectra of all samples were recorded at room temperature.

Visible Raman spectroscopy

Visible Raman spectra were recorded on a Jobin-Yvon U1000 scanning double monochromator with the spectrum resolution of 4 cm^{-1} using radiation of 488 and 514.5 nm from an argon ion laser (Spectra Physics) and 532 nm from a Coherent DPSS 532 Model 200 532 nm single-frequency laser, which is a diode-pumped, frequency-doubled Nd : YAG laser. The Raman signal was collected with 90° geometry. The spectra of all samples were recorded at room temperatures.

Ultraviolet–visible diffuse reflectance spectroscopy

UV–Vis diffuse reflectance spectra were recorded on a JASCO V-550 UV–Vis spectrophotometer.

XRD

XRD patterns were collected on a Rigaku Rotaflex (RU-200B) powder diffractometer equipped with a Cu target and an Ni filter.

Preparation of ZrO_2, SO_4^{2-}/ZrO_2 and Y_2O_3–ZrO_2

$Zr(OH)_4$ was obtained by adding aqueous ammonia slowly to the solution of zirconium oxychloride at room temperature with stirring until the pH of the solution reached ~10. The precipitate thus obtained was washed thoroughly with distilled water until chloride ions were not detected, and was then dried at 110 °C for 12 h. The dried precipitate sample was calcined at different temperatures for 2 h.

Yttrium-doped hydrated zirconium (Y_2O_3–ZrO_2) was obtained by coprecipitating a mixed solution of zirconium oxychloride and yttrium chloride at room temperature. The precipitate thus obtained was washed thoroughly with distilled water until chloride ions were not detected and then dried at 110 °C for 12 h. The dried precipitate was calcined at different temperatures for 2 h. The yttrium content of the solids was 2 mol% Y_2O_3–ZrO_2.

SO_4^{2-}/ZrO_2 was prepared by impregnating $Zr(OH)_4$ with 0.5 M H_2SO_4. Dried $Zr(OH)_4$ was impregnated with a large excess of H_2SO_4 [15 ml of H_2SO_4 per gram of $Zr(OH)_4$] for 2 h with stirring, then filtered. The solid was dried for 24 h at 100 °C. The dried sample was calcined at different temperatures for 2 h. The sulfur content of the solids was theoretically about 20 wt% for wet $SO_4^{2-}/Zr(OH)_4$. After the calcinations, the sulfur content was far below 20 wt%. The samples were not characterized by elemental analysis.

$Zr(OH)_4$ is in an amorphous phase and it can be converted into the tetragonal and monoclinic phase of ZrO_2 after the calcination at high temperatures.

RESULTS AND DISCUSSION

Change of ZrO_2 from tetragonal to monoclinic phase

Figure 1 shows the UV Raman spectra of powder samples of ZrO_2 calcined at different temperatures. When the sample was calcined at 350 °C, only a broad background is observed, suggesting the sample is amorphous. When the sample was calcined at 400 °C, the Raman spectrum gives major bands at 181, 270, 315, 472 and 631 cm^{-1}, which are characteristic bands of t-ZrO_2, except for the band at 181 cm^{-1}, due to the monoclinic phase.[34] The peaks at 178 and 190 cm^{-1} are not clearly separated owing to the low resolution for UV Raman spectroscopy, so only a single peak at 181 cm^{-1} is observed. The amorphous zirconia is transferred into t-ZrO_2after calcination at 400 °C. The striking differences in the Raman spectra between the tetragonal and monoclinic phases of ZrO_2 are as follows. The Raman bands at 149, 269 and 312 cm^{-1} are exclusively assigned to the tetragonal phase of ZrO_2 and the bands at 181 and 337 cm^{-1} are assigned to the monoclinic phase. The bands at 472 and 631 cm^{-1} are common for both phases but the relative intensity is different for the two phases. For the tetragonal phase, the intensities of the bands at 472 and 631 cm^{-1} are about the same or slightly stronger for the band at 631 cm^{-1}, but the intensity of the band at 472 cm^{-1} is much stronger than that of the band at 631 cm^{-1} for the monoclinic phase. Further, there are some small bands in between 472 and 631 cm^{-1} for the monoclinic phase, but these weak bands are absent for the tetragonal phase. Obviously, the UV Raman spectrum (Fig. 1) of the sample calcined at 400 °C is mainly due to the t-ZrO_2 phase together with a relatively minor proportion of m-ZrO_2.

When the sample was calcined at 500 °C, the Raman bands due to t-ZrO_2 (269 and 315 cm^{-1}) disappear, as shown in Fig. 1, while the bands of m-ZrO_2 (181, 305, 335, 378 cm^{-1}) are observed. The UV Raman spectrum clearly shows that the sample changes into the monoclinic phase after calcination at 500 °C. The Raman bands of the monoclinic phase increase in intensity further when the sample was calcined at 600 and 700 °C (see Fig. 1), indicating that the monoclinic phase becomes predominant when the zirconia is calcined at higher temperatures.

Figure 2 shows the XRD patterns of the zirconia samples calcined at different temperatures. When the sample was calcined at 350 °C, the diffraction peaks due to the crystalline phase are not observed. This suggests that ZrO_2 is in an amorphous phase. When the sample was calcined at 400 °C, the diffraction peaks are mainly from the tetragonal phase. Both the tetragonal and cubic phases give a broad diffraction peak at $2\theta = 30°$, and this makes the discrimination between the two phases difficult by XRD.[35] The Raman spectra and the number of Raman bands for the tetragonal and cubic phases of zirconia are completely different.[35] From Fig. 1, the bands due to the cubic phase are not observed. A small portion of ZrO_2 may still remain as an amorphous phase because the XRD peaks are somewhat broad. This means that the zirconia is mainly in the tetragonal phase after calcination at 400 °C, but this is inconsistent with the results from the UV Raman spectra (Fig. 1). The diffraction peaks of t-ZrO_2 decline and the peak intensities of m-ZrO_2 increase when the sample was calcined at 500 °C. However, the XRD peaks of t-ZrO_2 are still very strong, indicating that the t-ZrO_2 phase is still a major fraction in the zirconia. In contrast, the UV Raman spectra (Fig. 1) suggest that zirconia is nearly all in the monoclinic phase. When the sample was calcined at 600 and 700 °C, the diffraction peaks of m-ZrO_2 become more predominant and those of t-ZrO_2 gradually become weak.

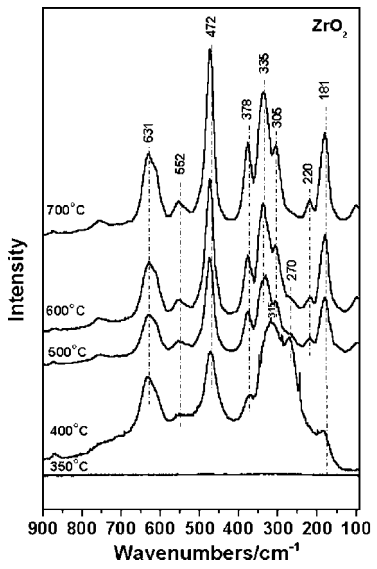

Figure 1. UV Raman spectra of ZrO_2 calcined at 400, 500, 600 and 700 °C. Initial sample, $Zr(OH)_4$; laser excitation, 244 nm.

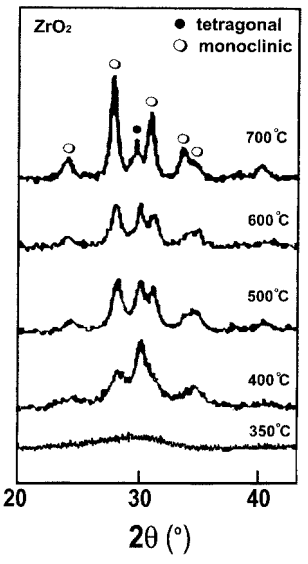

Figure 2. XRD patterns of ZrO_2 calcined at 400, 500, 600 and 700 °C. Initial sample, $Zr(OH)_4$; $2\theta = 29, 34°$for tetragonal phase and 25, 28, 31, 33, 35°for monoclinic phase.

JRS

The XRD patterns suggest that some t-ZrO_2 phase still exists even after the sample was calcined at 600 and 700 °C.

By comparing Figs 1 and 2, it can be seen that there are some discrepancies between the results from UV Raman spectroscopy and XRD. According to the UV Raman spectra, m-ZrO_2 is the main phase after the sample was calcined at 500 °C, but the results from XRD indicate that t-ZrO_2 is still the major part of the zirconia after calcination at 500 °C. The tetragonal phase of zirconia can be detected by XRD even after the calcination at 600 and 700 °C, whereas the UV Raman spectra only show the monoclinic phase when the calcination temperature is above 500 °C.

Figure 3 shows the Raman spectra excited with visible light for zirconia samples calcined at different temperatures. The Raman bands of t-ZrO_2 at 146, 268 and 316 cm^{-1} are dominant in the spectrum, and the band at 640 cm^{-1} is stronger than that at 476 cm^{-1}. Apparently, zirconia is mainly in the tetragonal phase after calcination at 400 °C. This is in agreement with the UV Raman spectrum (Fig. 1) and XRD pattern (Fig. 2). When the sample was calcined at 500 °C, the intensities of the bands at 175, 186, 333 and 379 cm^{-1} attributed to m-ZrO_2 increase whereas the bands at 146, 268 and 316 cm^{-1} are still comparable in intensity with those of the sample calcined at 400 °C. This suggests that the portion of m-ZrO_2 phase in zirconia is increased, but there is still a considerable amount of t-ZrO_2. For the sample calcined at 600 °C, the Raman bands at 175, 186, 220, 303, 333, 342, 379, 615 and 634 cm^{-1} together with those at 535 and 556 cm^{-1} due to monoclinic phase become relatively stronger. However, the Raman bands at 146 and 268 cm^{-1} due to the characteristic bands of t-ZrO_2 are still observed. This strongly indicates that some tetragonal phase remains, although the major part of the sample is in the monoclinic phase. The Raman bands of tetragonal phase become very weak only after the sample was calcined at 700 °C and above. Interestingly, all these results from visible Raman spectroscopy are in good agreement with the results from XRD (Fig. 2) but different to those from UV Raman spectroscopy.

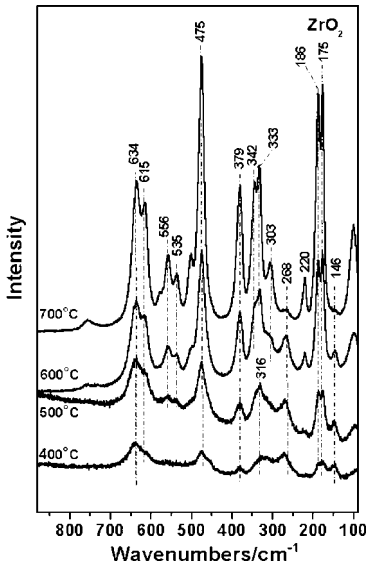

Figure 3. Visible Raman spectra of ZrO_2 calcined at 400, 500, 600 and 700 °C. Initial sample, $Zr(OH)_4$; laser excitation, 532 nm.

For solid samples, Raman scattering comes from both the surface and the bulk of the solids. However, the signal from the bulk is attenuated, particularly when the sample strongly absorbs the excitation laser light and the scattering light. Therefore, more Raman scattering comes from the surface top region than from the bulk of a solid sample when the sample absorbs the excitation laser light. In particular, most transition metal oxides strongly absorb UV laser light, so UV Raman spectroscopy is more sensitive to the surface region than to the bulk for these samples. Visible Raman spectroscopy usually gives information from both the bulk and the surface of a sample because there is no electronic absorption in the visible region for most samples.

UV–Vis diffuse reflectance spectra of zirconia (ZrO_2), sulfated zirconia (SO_4^{2-}/ZrO_2) and yttrium oxide-doped zirconia ($Y_2O_3–ZrO_2$) show a strong band centered at 230 nm. The laser radiation used as the excitation in this work was at 244 nm, which is near to the electronic absorption of ZrO_2, SO_4^{2-}/ZrO_2 and $Y_2O_3–ZrO_2$. Accordingly, the phase transformation in the surface region of these samples could be detected selectively by UV Raman spectroscopy. In contrast, XRD and visible Raman spectroscopy give information on both the surface region and the bulk, so the conclusions drawn from the two methods are in accord each other but not consistent with UV Raman spectroscopy. It is difficult to separate the information of the surface phase from the bulk phase of ZrO_2, SO_4^{2-}/ZrO_2 and $Y_2O_3–ZrO_2$ using visible Raman spectroscopy and XRD, because there is no electronic absorption in the visible region for these materials.

The m-ZrO_2 phase is sensitively detected by UV Raman spectroscopy when zirconia is calcined at relatively lower temperatures compared with that detected by XRD and visible Raman spectroscopy. The disagreement between the results from UV Raman spectroscopy and those from XRD and visible Raman spectroscopy can be interpreted in terms of the phase transformation of zirconia starting from the surface region and then progressing to the bulk. The initial change of the phase at the surface region can be sensitively detected by UV Raman spectroscopy but not by XRD and visible Raman spectroscopy.

When amorphous $Zr(OH)_4$ is calcined at elevated temperatures, tetragonal zirconia is first formed at about 400 °C; meanwhile, a small part of the tetragonal zirconia begins to change into the monoclinic phase in the surface region at this temperature as detected by UV Raman spectroscopy. The whole bulk is in the tetragonal phase at 400 °C, as confirmed by XRD and visible Raman spectroscopy. When the calcination temperature is over 500 °C, the UV Raman spectra show only the bands of the monoclinic phase, indicating

that the whole surface region is in the monoclinic phase and the thickness of the surface layer of the monoclinic phase is gradually increased with increase in temperatures. The results from XRD and visible Raman spectroscopy reveal that the tetragonal phase of zirconia can be detected even after calcination at 600 and 700 °C. This leads us to conclude that the tetragonal phase starts to change into the monoclinic phase at the surface region and then the phase transformation progressively develops into the bulk.

Phase change of Y_2O_3–ZrO_2 at elevated temperatures

Figure 4 shows the UV Raman spectra of Y_2O_3–ZrO_2 calcined at temperatures from 500 to 800 °C (the spectrum for the sample calcined at 400 °C is not shown because this sample is amorphous). These spectra are slightly different from those of ZrO_2, possibly because of the presence of Y_2O_3. From the bands at 303, 340 and 374 cm^{-1} together with the relative intensities of the bands at 476 and 630 cm^{-1}, the surface region of Y_2O_3–ZrO_2 is mainly in the monoclinic phase after calcination at 500 °C. Surprisingly, the UV Raman spectra hardly change for the sample calcined at different temperatures even up to 800 °C.

Figure 5 presents the XRD patterns of the Y_2O_3–ZrO_2 samples calcined at elevated temperatures. When the sample was calcined at 400 °C, the diffraction peaks of the crystalline phases are not observed. The XRD pattern ($2\theta = 30, 35°$) of the sample calcined at 500 °C is due to t-ZrO_2. The sample is mainly in the tetragonal phase after calcination at 600 °C, except for a tiny peak at $2\theta = 28°$ due to the monoclinic phase. When the sample is calcined at 700 °C, some weak peaks of the monoclinic phase are observed, while the main pattern is due to the tetragonal phase. The major part of the tetragonal phase can be maintained up to 800 °C and

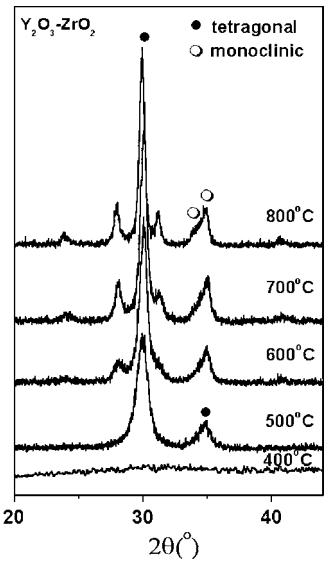

Figure 5. XRD patterns of Y_2O_3–ZrO_2 calcined at 400, 500, 600 and 700 °C. $2\theta = 29.5, 34.5°$ for tetragonal phase, and 25, 34, 35° for monoclinic phase.

the peaks of the monoclinic phase are not increased very much with calcination temperatures from 600 to 800 °C. This is strong evidence that the tetragonal phase of zirconia can be stabilized by adding yttrium oxide or forming a solid solution of Y_2O_3–ZrO_2, although its phase in the surface region is easily changed into the monoclinic form.

Figure 6 shows the near-UV Raman spectra of Y_2O_3–ZrO_2 calcined at temperatures from 500 to 800 °C with laser excitation at 325 nm (it was intended to record the visible Raman spectra using 514.5 or 488 nm radiation, but strong fluorescence obscures the Raman signal). The Raman spectrum for

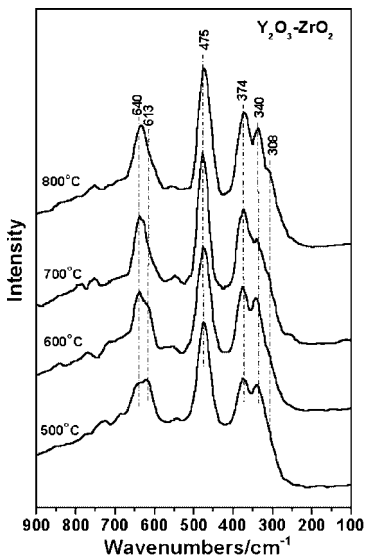

Figure 4. UV Raman spectra of Y_2O_3–ZrO_2 calcined at 500, 600, 700 and 800 °C. Laser excitation, 244 nm.

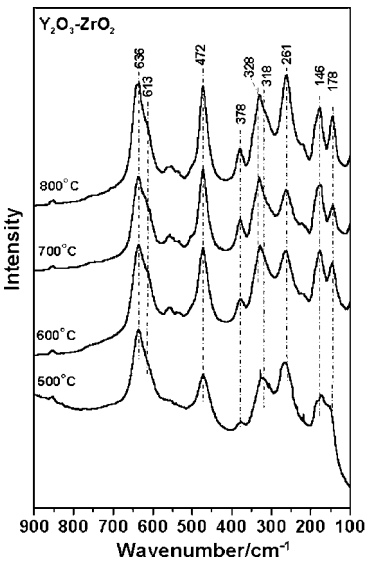

Figure 6. Near-UV Raman spectra of Y_2O_3–ZrO_2 calcined at 500, 600, 700 and 800 °C. Laser excitation, 325 nm.

JRS

the sample calcined at 500 °C gives the characteristic bands of t-ZrO_2 at 146, 261 and 318 cm^{-1}. In addition, the intensity ratio between the bands at 472 and 636 cm^{-1} also suggests that the sample is mainly in the tetragonal phase. Karlin and Colomban[36] observed the wavenumber shift in germanium-doped ZrO_2 that is due to shortening of the Zr—O bonds. They also proposed that the shortening of the Zr—O bonds is the origin of the stabilization of the tetragonal phase. The fact that the Raman spectra of Y_2O_3–ZrO_2 (Figs 4 and 6) are slightly different from those of ZrO_2 (Figs 1 and 3) reveals that the Y_2O_3–ZrO_2 is in a solid solution state or that some zirconium atoms are substituted by yttrium atoms in Y_2O_3–ZrO_2.

From Fig. 6, it is clearly seen that the Raman spectra recorded for the samples calcined at 600, 700 and 800 °C are essentially the same as that for the sample calcined at 500 °C. Some weak bands at 178, 378 and ~540 cm^{-1} due to the monoclinic phase appear and slightly develop at elevated calcination temperatures. The major feature of the spectra indicates that the Y_2O_3–ZrO_2 sample retains its tetragonal phase even after the calcination at 800 °C. The Raman spectra recorded with laser excitation at 325 nm reflect the phase of the bulk because the electronic absorption near 325 nm is very small. The Raman spectra obtained with laser excitation at 325 nm is totally different from those with the excitation at 244 nm, but the conclusion is same as that from XRD.

The remarkable difference in the results of UV Raman spectroscopy, near-visible Raman spectroscopy and XRD leads us to the conclusion that the different techniques take the signals from different parts of the solid particle. The fact that the UV Raman spectra show only information on the monoclinic phase indicates that the surface region of the sample is mainly in the monoclinic phase. However, from the XRD patterns and near-visible Raman spectra, the bulk of the sample is in the tetragonal phase. This substantiates that the phase transformation from tetragonal to monoclinic starts from the surface region. It turns out that the tetragonal phase of Y_2O_3–ZrO_2 at the surface region is easily converted into the monoclinic phase when the calcination temperature is above 400 °C. However, the tetragonal phase of Y_2O_3–ZrO_2 in the bulk is considerably more stable compared with ZrO_2 alone (see Figs 1, 2 and 3). Based on the UV Raman spectra and XRD patterns, it can be assumed that a thin layer of monoclinic phase is formed in the surface region of a particle and the monoclinic shell does not extend into the bulk owing to the presence of yttrium oxide.

The phase change of SO_4^{2-}/ZrO_2 at elevated temperatures

Figure 7 exhibits the UV Raman spectra of sulfated zirconia (SO_4^{2-}/ZrO_2) after calcination at 500, 600, 700 and 800 °C. The left panel shows the Raman spectra of zirconia itself and the right panel mainly those for surface sulfated groups. The Raman bands for the sample calcined at 500 °C are not clearly observed, probably because the sample is still amorphous

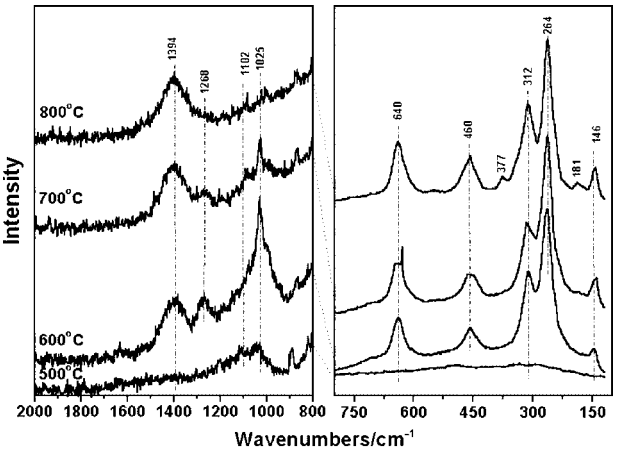

Figure 7. UV Raman spectra of SO_4^{2-}/ZrO_2 calcined at 500, 600, 700 and 800 °C. Laser excitation, 244 nm.

and because of fluorescence interference. Obviously the Raman bands at 146, 264, 312, 460 and 640 cm^{-1} in the left panel are due to tetragonal zirconia and these bands are unchanged even after calcination at 800 °C. This suggests that the sulfated zirconia can retain its tetragonal phase up to relatively high temperatures. The right part of Fig. 7 shows bands at 1025, 1102, 1268 and 1394 cm^{-1}, which are attributed to the symmetric and asymmetric vibrations of surface sulfated groups (such as $SO_4^{2-}{}_{ads}$). These bands change in intensity with increase in calcination temperature, but the band at 1394 cm^{-1} still remains. Accordingly, the high stability of the tetragonal phase must be partly due to the presence of the surface sulfated groups.

Figure 8 shows the UV Raman spectra of sulfated zirconia (SO_4^{2-}/ZrO_2) after calcination at 500, 600, 700 and 800 °C, but the sample was thoroughly ground before making the sample disc for the UV Raman and XRD measurements

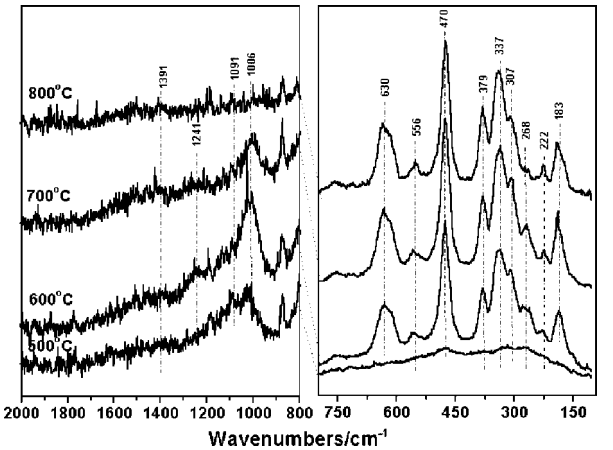

Figure 8. UV Raman spectra of SO_4^{2-}/ZrO_2 calcined at 500, 600, 700 and 800 °C. Laser excitation, 244 nm. The samples are those after the XRD measurement, and these samples were ground before making the disc for XRD.

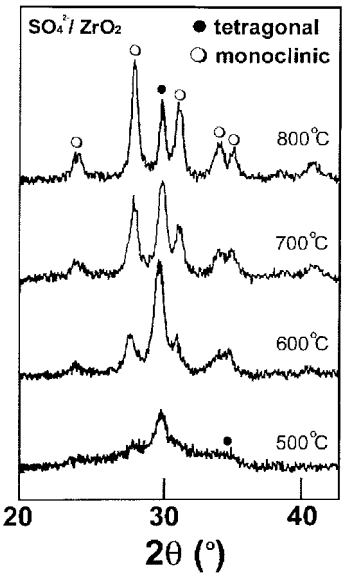

Figure 9. XRD patterns of SO_4^{2-}/ZrO_2 calcined at 500, 600, 700 and 800 °C. The sample was ground before making a disc for XRD measurement.

(Fig. 9). This is different from Fig. 7, where the sample was not ground before the UV Raman measurement. It is interesting that the UV Raman spectra are dramatically different from those in Fig. 7. The Raman bands at 183, 222, 307, 337, 379 and 556 cm^{-1} belong to m-ZrO_2 and the weak band at 268 cm^{-1} is from the tetragonal phase. The zirconia already changes into the monoclinic phase at least in the surface region at 600 °C. The monoclinic phase is found after the sample was violently ground (Fig. 8). This is because grinding could affect the sulfate groups (the band at 1394 cm^{-1} disappears). The tetragonal phase is stabilized by the surface sulfate groups for the SO_4^{2-}/ZrO_2 sample. In addition, Stefanic *et al*.[37] proposed that ball-milling occasionally transfers sufficient energy to a small part of a grain to cause the phase transformation. The concentration of energy on a small part of a grain could lead to a change in particle size. Hence the facile transformation of zirconia from the tetragonal to the monoclinic structure is attributed solely to the grinding which may produce large changes in the particles size, sulfated groups and the texture of the zirconia particle. The Raman spectra of sulfated groups are also different from those without grinding. The Raman bands at 1390 cm^{-1} region disappear even for the sample calcined at 500 °C and all the Raman bands are absent for the sample calcined at 800 °C. The change in the sulfated groups may result in the phase change from tetragonal to monoclinic or, in other words, the tetragonal phase is stabilized by the surface sulfated groups.

XRD patterns of the SO_4^{2-}/ZrO_2 samples calcined at different temperatures were also recorded after the samples were ground (Fig. 9). For the sample calcined at 500 °C, the broad peaks of the tetragonal phase are detected, indicating that the sample is just an intermediate from amorphous to tetragonal phase. The peaks of the tetragonal phase become stronger when the sample is calcined at 600 °C, and the peaks of monoclinic phase are observed. The peak intensities of the monoclinic phase grow steadily as those of the tetragonal phase decline with increase in calcination temperatures. For the sample calcined at 800 °C, the monoclinic phase is predominant but the peaks of tetragonal phase are still fairly strong. This suggests that the phase transformation from tetragonal to monoclinic can be considerably retarded for SO_4^{2-}/ZrO_2 compared with ZrO_2 (see Figs 2–4).

The grinding of the sample may make the particle size smaller and lead to the destruction of surface sulfated groups. The grinding process may induce a phase change in the surface region since the UV Raman spectrum of the sample after calcination at 500 °C shows the monoclinic phase. This is also a possible reason for the scattered and inconsistent results reported in the literature.

Figure 10 describes schematically the phase evolution of the ZrO_2, SO_4^{2-}/ZrO_2 and Y_2O_3–ZrO_2 at elevated calcination temperatures. The phase transformation from tetragonal to monoclinic begins at the surface region and then possibly extends into the bulk until the whole particle becomes the monoclinic phase. For ZrO_2, the phase change from tetragonal to monoclinic starts even at 400 °C and the phase becomes totally monoclinic at about 700 °C. For SO_4^{2-}/ZrO_2, the phase transformation is slowed and its tetragonal phase can be stabilized in the bulk even after the sample is calcined at 800 °C. This is due to the surface sulfated groups, which can prevent the phase in the surface region from undergoing transformation. When the surface sulfated groups are removed or decomposed, the phase changes more easily. The tetragonal phase of Y_2O_3–ZrO_2 solid solution is very stable because of the presence of Y_2O_3 although its phase in the surface region is easily converted into the monoclinic phase. This surface layer of monoclinic phase hardly extends further into the bulk so that the tetragonal phase in the bulk can be stable up to 800 °C.

CONCLUSION

The changes of ZrO_2, SO_4^{2-}/ZrO_2 (sulfated ZrO_2) and Y_2O_3–ZrO_2 (yttrium doped ZrO_2) from the tetragonal to the monoclinic phase were characterized by UV Raman spectroscopy. UV Raman spectroscopy is particularly sensitive to the surface region of ZrO_2 because ZrO_2 absorbs UV radiation. It is found that the phase change of ZrO_2 begins from the surface region or the skin of ZrO_2 and then develops progressively into its bulk. The phase change of sulfated ZrO_2 is significantly retarded because of the presence of surface sulfate groups. Consequently, the tetragonal phase of SO_4^{2-}/ZrO_2 can be stabilized to a higher temperature compared with ZrO_2 itself. This can be interpreted in terms of the stable structure formed between the sulfate groups and the surface of ZrO_2 with a tetragonal structure. After doping

JRS

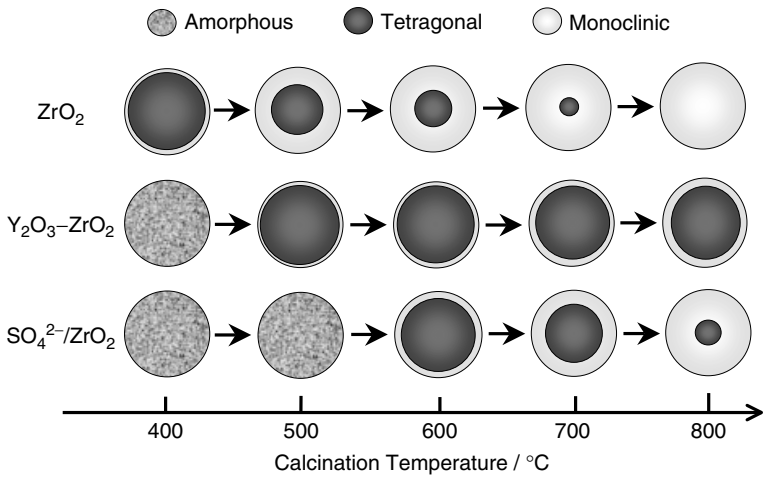

Figure 10. Schematic description of the phase transformation of ZrO_2, SO_4^{2-}/ZrO_2 and $Y_2O_3-ZrO_2$ calcined at elevated temperatures.

yttrium oxide into ZrO_2, the phase change at the surface region is not apparently retarded, but the further development into bulk is slowed substantially. The tetragonal phase of the bulk is stabilized by adding yttrium oxide but the tetragonal phase in the surface region cannot be stabilized. A possible reason for this is that a solid solution of $Y_2O_3-ZrO_2$ may be formed only in the bulk and not in the surface region.

Acknowledgements

This work was financially supported by the Natural Science Foundation of China (NSFC, Grants 29625305, 20073045) and the State Key Project for Basic Research from the Ministry of Science and Technology (Grant G1999022407). Colleagues partly involved in this work were Guang Xiong, Zhaochi Feng, Pinliang Ying and Qin Xin.

REFERENCES

1. Stencel JM. *Raman Spectroscopy for Catalysis*. Van Norstrand Reinhold: New York, 1990.
2. Campion A. In *Vibrational Spectroscopy of Molecular on Surfaces*, Yates JT Jr, Madey TE (eds). Plenum Press: New York, 1987; 345.
3. Brown FR, Maskovsky LE, Rhee KH. *J. Catal.* 1977; **50**: 162.
4. Brown FR, Maskovsky LE, Rhee KH. *J. Catal.* 1977; **50**: 385.
5. Brown FR, Maskovsky LE. *Appl. Spectrosc.* 1977; **31**: 44.
6. Knopps-Gerrits PP, Vos De DE, Feijen EJP, Jacobs PA. *Microporous Mater.* 1997; **8**: 3.
7. Li C, Stair PC. *Stud. Surf. Sci. Catal.* 1996; **101**: 881.
8. Li C, Stair PC. *Catal. Lett.* 1996; **36**: 119.
9. Li C, Stair PC. *Stud. Surf. Sci. Catal.* 1997; **105**: 599.
10. Li J, Xiong G, Feng ZC, Liu Z, Xin Q, Li C. *Micro. Meso. Mater.* 2000; **39**: 275.
11. Xiong G, Li C, Li HY, Xin Q, Feng ZC. *J. Chem. Soc., Chem. Commun.* 2000; 677; Li C, Xiong G, Xin Q, Liu J, Ying PL, Feng ZC, Li J, Yang W, Wang Y, Wang G, Liu X, Liu M, Wang X, Min E. *Angew. Chem., Int. Ed. Engl.* 1999; **38**: 2220.
12. Xiong G, Li C, Feng ZC, Ying PL, Xin Q, Liu J. *J. Catal.* 1999; **186**: 234.
13. Xiong G, Feng ZC, Li J, Yang H, Ying PL, Xin Q, Li C. *J. Phys. Chem. B* 2000; **104**: 3581.
14. Stair PC, Li C. *J. Vac. Sci. Technol.* 1997; **A15**: 1679.
15. Srinivasan R, Davis BH. *Catal. Lett.* 1992; **14**: 165.
16. Štefanić G, Musić S, Gržeta B, Popović S, Sekulić A. *J. Phys. Chem. Solids* 1998; **59**: 879.
17. Xia B, Duan LY, Xie YCH. *J. Am. Chem. Soc.* 1983; **5**: 1077.
18. Su S, Bell AT. *J. Phys. Chem. B* 1998; **102**: 7000.
19. Dang Z, Anderson BG, Amenomiya Y, Morrow BA. *J. Phys. Chem.* 1995; **99**: 14437.
20. Miller JM, Lakshmi J. *J. Phys. Chem. B* 1995; **102**: 6465.
21. Pacheco G, Fripiant JJ. *J. Phys. Chem. B* 2000; **104**: 11906.
22. Štefanić II, Musić S, Štefanić G, Gajović A. *J. Mol. Struct.* 1999; **480-481**: 621.
23. Comelli RA, Vera CR, Parera JM. *J. Catal.* 1995; **151**: 96.
24. Sekulic A, Furic K. *J. Mater. Sci. Lett.* 1997; **16**: 260.
25. Hirata T, Asari E, Kitajima M. *J. Solid State Chem.* 1994; **110**: 201.
26. Garvie RC. *J. Phys. Chem.* 1965; **69**: 1238.
27. Djurado E, Bouvier P, Lucazeau G. *J. Solid State Chem.* 2000; **149**: 399.
28. Murase Y, Kato E. *J. Am. Ceram. Soc.* 1982; **66**: 196.
29. Mirgorodsky AP, Smirnov MB, Quintard PE. *Phys. Rev. B* 1997; **55**: 19.
30. Neigita K, Takao H. *J. Phys. Chem. Solids* 1989; **50**: 325.
31. Somiya S, Yamamoto N, Yanagida H. Science and Technology of Zirconia III. Advances in Ceramics. 1986; 24A and 24B.
32. Srinivasan R, Taulbee D, Davis BH. *Catal. Lett.* 1991; **9**: 1.
33. Haase F, Sauer J. *J. Am. Chem. Soc.* 1998; **120**: 13 505.
34. Shi L, Tin K, Wong N. *J. Mater. Sci.* 1999; **34**: 3367.
35. Berry FJ, Skinner SJ, Bell IM, Clark RJH, Ponton CB. *J. Solid State Chem.* 1999; **145**: 394.
36. Karlin S, Colomban P. *J. Am. Ceram. Soc.* 1999; **82**: 735.
37. Stefanic G, Music S, Sekulic A. *Thermochim. Acta* 1996; **273**: 119.